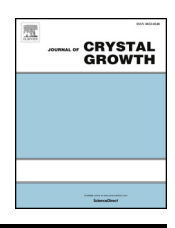
ELSEVIER

Contents lists available at ScienceDirect

Journal of Crystal Growth

journal homepage: www.elsevier.com/locate/jcrysgro



Growth of high purity zone-refined Boron Carbide single crystals by Laser Diode Floating Zone method



Michael Straker^{a,*}, Ankur Chauhan^{b,c}, Mekhola Sinha^d, W. Adam Phelan^d, M.V.S. Chandrashekhar^e, Kevin J. Hemker^{b,c}, Christopher Marvel^h, Michael Spencer^{f,g}

- ^a Department of Physics and Engineering Physics, Morgan State University, Baltimore, MD 21251, USA
- ^b Department of Mechanical Engineering, The Johns Hopkins University, Baltimore, MD 21218, USA
- ^c Hopkins Extreme Materials Institute, The Johns Hopkins University, Baltimore, MD 21218, USA
- ^d Department of Chemistry, The Johns Hopkins University, Baltimore, MD 21218, USA
- ^e Department of Electrical Engineering, University of South Carolina, Columbia, SC 29208, USA
- f Department of Electrical and Computer Engineering, Morgan State University, Baltimore, MD 21251, USA
- g Department of Electrical and Computer Engineering (Emeritus), Cornell University, Ithaca, NY 14853, USA
- h Department of Material Science and Engineering, Lehigh University, Bethlehem, PA 18015, USA

ARTICLE INFO

Communicated by Matthias Bickermann

Keywords:

A1. Characterization A1. X-ray diffraction

A1. Defects

A2. Single crystal growth

A2. Growth from melt

ABSTRACT

We report the growth of 4 mm diameter \times 50 mm long Boron Carbide (B₄C) with large single crystal regions using a Laser Diode Floating Zone (LDFZ) method at varying growth rates of 5–20 mm/hr. These materials were grown using polycrystalline B₄C as a seed. Microstructural characterization shows the presence of a significant number of twinning-boundaries along the growth direction ([0 0 1]_h) oriented in the (1 2 1 0)_h plane. At faster growth rates > 10 mm/hr, the crystal orientation was reproducible, suggesting a twin-plane mediated growth mechanism. On the contrary, at slower growth rates < 10 mm/hr the crystal orientation was not reproducible, suggesting a critical rate for twin-plane mediated growth to dominate. Zone refinement of these crystals led to a significant reduction of trace impurities to better than 99.999 wt% purity, at the expense of increased twinning. Powder x-ray diffraction confirms that the bulk is rhombohedral B₄C, consistent with the microstructural analysis. The X-ray reciprocal space maps reveal the growth direction to be close to the [0 0 1]_h direction, and the corresponding ω -rocking curve width is \sim 530 arcsec. The rocking curve consisted of 3 distinct peaks, indicating in-plane mosaicism, consistent with the twinning observed. Berkovich nano-indentation of the key (0 0 1)_h plane showed 41 \pm 1 GPa hardness, with a Young's modulus of 520 \pm 14 GPa, comparable to literature reports.

1. Introduction

Boron carbide (B_4C) is a key material used in protection applications during high impact situations due to its low cost, low density, high hardness (\sim 40GPa), and high stiffness (elastic modulus > 500GPa) [10]. Being the hardest material after diamond and c-BN [11], it is ideal for applications where extreme mechanical stresses need to be managed. The high strength of armor composites made from B_4C is often attributed to its icosahedral structure [11]. The boron icosahedra are connected by sp³ chains of boron and carbon atoms to form the B_4C structure. Similar icosahedral boron materials have been proposed for applications, where self-healing at the atomic level is desirable.

Despite the need for engineering composites based on B_4C , and the numerous studies characterizing mechanical failure in these composites [7,4,5], there are few studies on the mechanical properties of single

crystal B_4C [17,10]. B_4C is highly anisotropic, with measured elastic moduli varying by as much as 10x between different crystallographic orientations [17]. Given this anisotropy, it is critical to obtain high purity single crystals to completely characterize the elastic moduli, hardness, and dynamic failure mechanisms along various crystal planes. This information can be used in constitutive computer models of B_4C mechanical failure [8]. For these models to have predictive power for rational material design the mechanical properties as a function of crystal orientation should be determined with a high degree of confidence

Gunjishima et al. [13] grew single crystal B_4C using a Xe-furnace float zone (FZ) method and characterized the electrical and thermoelectric properties along the basal (0 0 1)_h plane. Domnich [10] has characterized the hardness and modulus of the (0 0 1)_h and (1 0 1)_h planes and found no obvious anisotropy for those two planes. Given

E-mail address: mistr2@morgan.edu (M. Straker).

^{*} Corresponding author.

that B_4C has a rhombohedral crystal structure, the determination of six independent crystal directions are needed to completely resolve the mechanical anisotropy of the crystal, [9]. The work of McLellan et al. [17] on the elastic moduli of FZ grown B_4C provides valuable insight to the anisotropy of this unique material, although there is still ambiguity in the interpretation of the data because the software used to fit that data did not use the rhombohedral structure. To resolve this question, well-oriented high purity single crystals are needed to explicitly measure the elastic anisotropy along the key crystal planes.

In this paper, we demonstrate for the first time that well-oriented B_4C single crystals can be grown using a Laser-Diode Floating Zone (LDFZ) method. This technique is similar to Xe-furnace techniques used by other researchers [11], with the advantage of better control of the molten zone and temperature gradients [14]. LDFZ is a relatively new technique requiring the target material to be strongly absorbing at the laser wavelength. B_4C , a congruently melting material, is absorbing at the laser wavelengths used during crystal growth. It is therefore an ideal candidate material for LDFZ growth. In LDFZ growth, a laser melts the polycrystalline feed material, small single crystals spontaneously nucleate, and the initial nuclei crystals begin to expand. Due to the anisotropy of the crystal, one direction appears to grow faster, eventually becoming dominate at which point large area single crystal regions are achieved.

We report on the successful application of zone-refinement to reduce impurity levels to better than 99.999% purity.

2. Experimental methods

2.1. Crystal growth

Boron carbide powder was hot-pressed into dense 10 mm long 6 mm diameter rods by a commercial vendor. These rods were loaded into a LDFZ furnace. To initiate the growth process, the top of the lower rod (seed rod) was melted. After melting of the seed rod, the upper rod (feed rod) was slowly connected to the molten portion of the seed to form a molten/floating zone, as shown in Fig. 1a. The seed and feed were counter-rotated at 10 rpm to ensure adequate mixing of the material during growth. Upon formation of a stable, well-defined molten zone, the rods were translated downward at rates of 5-20 mm/hr to nucleate and grow the single crystal. The stability of these lasers, and their ability to be positioned precisely provides a highly controllable heat source. In the LDFZ furnace, five GaAs (Gallium Arsenide) laser diodes surround the seed and feed rods emitting 1 kW of localized laser power at a wavelength of 975 nm. The laser power is slowly increased over to avoid thermal shocking of the material. The heating profile is set to increase from 0 to 80% laser power over a 1 hr period and is

manually stopped once a stable molten zone is achieved. A stable molten zone was reproducibly established between $\sim\!80\%$ laser power.

The phase diagram of B_4C shows that at the eutectic point, a single-phase region with carbon content in the range of $\sim 17-20\%$ [3] exists. This region of the phase diagram is large, allowing for the potential creation of a wide range of boron carbide compositions. During the crystal growth vaporization and the formation of a skin on the feed rod above the molten zone were observed (Fig. 1a). Graphitic carbon has been shown in multiple studies to be produced [6,21,11]. Our Raman data show that the composition of this skin to be graphite, indicating that the composition of the vapor is boron rich. Single crystals of boron carbide (Fig. 1b), $\sim 7-8$ cm long were reproducibly obtained, with no graphitic inclusions in the center of the crystal (See supplementary results).

An aditional zone pass was performed on one of the grown crystal to illustrate that the overall purity of single crystals of boron carbide could be increased. Impurity levels could further be reduced with additional zone passes. In the zone refinement process, the LDFZ crystal growth process is repeated, using a single crystal grown at the same growth rate of 10 mm/hr as the feed and seed rods. When the molten zone is established, two solid liquid interfaces are created on either side. During growth as the molten zone moves up the crystal (feed rod) impurities are pulled into the molten zone and concentrate at either interface. This occurs due to the difference in solubility of these materials in the liquid and solid phases as characterized by the segregation coefficient ($k = c_s$ / c_l) where c_s represents solubility in the solid phase and c_l represents solubility in the liquid phase) as well as thermodynamic forces such as convection [18]. Materials with k > 1 will concentrate at the top of the molten zone. Materials with $k \ < \ 1$ will not be incorporated into the lattice of the resulting crystal formed below the interface and will ultimately settle in the last portion of the crystal to solidify. The repetition of this process results in a purer crystal [19] and is routinely used in semiconductor manufacturing to achieve ppb purity.

2.2. Characterization

Powder X-ray diffraction patterns were collected using a Bruker D8 Focus diffractometer with Cu-K α radiation (see supplementary information). Phase identification and unit cell determinations were carried out using the Bruker TOPAS software. A silicon standard was added to the B₄C powder as a reference to accurately determine lattice parameter. This was also used to identify the phase and estimate the B/C ratio by comparing the lattice constants produced by performing a Le Bail fit on the X-ray diffraction data to lattice constants appearing in the literature [1].

X-ray energy dispersive spectrometry (XEDS), as described in a

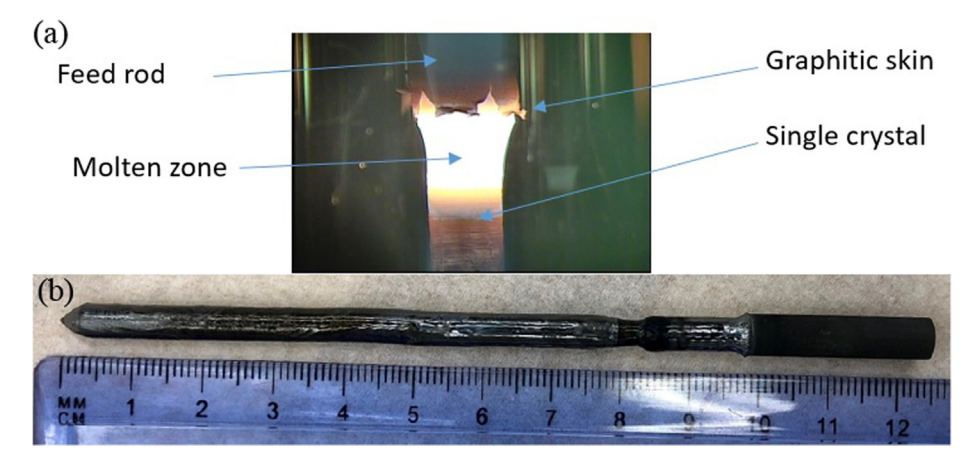


Fig. 1. Float Zone crystal growth of boron carbide. a) The figure shows the feed rod as it feeds material into the liquid molten zone resulting in the single crystal after it cools. b) Resulting crystal from a float zone crystal growth of Boron Carbide in the Laser Diode Floating Zone Furnace.

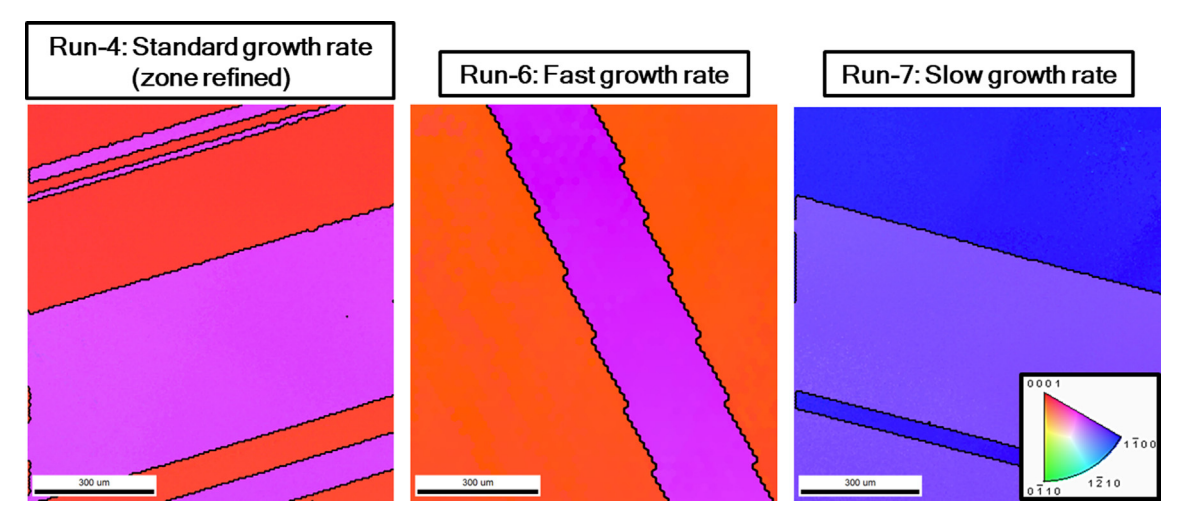


Fig. 2. EBSD orientation maps of boron carbide samples grown at varying growth rates. The angled purple areas in maps are twins. The color key is common for all of the samples. The step sizes for the EBSD scans were 5 μ m for the Run-4 (10 mm/hr) and Run-6 (20 mm/hr) samples and 20 μ m for the Run-7 (5 mm/hr) sample. The scale bar is 300 μ m for all samples.

paper by Marvel [16], was performed by collaborators at Lehigh on a sample of B_4C that had been cut and polished with diamond particles down to 0.1 μ m grit size to obtain the B/C ratio. Micro-Raman spectroscopy using a 473 nm laser was used to perform further chemical analysis to confirm that excess carbon phases [22] are removed from the cut surface. While the surface of the growing crystal graphitizes during growth (see supplementary information), this ~200 nm thick "skin" is only on the crystal edge, and not in the bulk of the crystal.

Backscattered white beam X-ray Laue diffraction with 1 mm spot size was utilized to check the orientations of the crystals in real-time. The resulting pattern was compared with a simulation of the crystal structure to identify and confirm the crystal direction. The crystals showed coherent Laue patterns over many centimeters (see supplementary information).

To further confirm the orientation of the grown crystals and to investigate their microstructure, electron backscattered diffraction (EBSD) and transmission electron microscopy (TEM) were carried out. Samples from multiple crystals grown at different growth rates were analyzed to investigate the effect of growth parameters on the crystal quality. For EBSD, the samples were cut with a slow speed diamond saw and mechanically polished to a mirror-like surface finish with diamond grit down to 0.1 μm . The Kikuchi patterns were recorded with a scanning electron microscope equipped with EDAX detector and with a step size of 5 μm , accelerating voltage of 20 kV and working distance of 20 mm. Post-processing of the acquired data was performed using analysis software. For TEM specimens, the samples were polished using a tripod polisher to create wedges and then further thinned down to electron transparency with ion milling.

The ω -rocking curves of the $[0\ 0\ 3]_h$ peak of B_4C polished single crystals were obtained with a triple-axis x-ray diffractometer with Cu-K α radiation. The reciprocal lattice map (RLM) was then obtained around this reflection to confirm the orientation of the crystal determined from EBSD and Laue above (see supplementary information).

Berkovich nano-indentation was used to determine the hardness and elastic modulus at maximum load of 50mN loads. In this method, a Berkovich-shaped diamond indenter applies a load to a sample then unloads while the displacement of the surface is measured. The hardness is obtained from the slope of the unloading curve, while Hooke's law is used to extract the elastic modulus [10].

A portion of each crystal was sent for commercial chemical analysis by glow discharge mass spectrometry (GDMS) for trace impurity quantification. In GDMS, ions of the material are released as a result of sputtering using the sample as cathode. These ions are analyzed by a mass spectrometer as a means of identification [15].

3. Results and discussion

The powder diffraction spectrum (see supplementary information) of a piece of the B₄C boule grown at 10 mm/hr was fit to the peaks with a Si-reference; giving the lattice constants of the B₄C crystal $a=5.60~\pm~7.74\times10^{-5}\,\mbox{\normalfont\AA}$ and $c=12.08~\pm~2.379\times10^{-4}\,\mbox{\normalfont\AA}$ for all the samples. From the calibration curves of Aselage et al. [1], this indicates a C-content of ~20%. There is also a broad Fe-peak that we believe is due to the stainless-steel mortar and pestle used to pulverize the B₄C and Si standard. Therefore, we exclude Fe as an impurity incorporated into the crystal during growth based on the GDMS chemical analysis (see supplementary information) and comparisons with XRD data from B₄C powder. The lattice constants derived from the X-ray powder diffraction data with a Le Bail fit (see supplementary information), show a carbon content of 19.25% and 19.50% for the standard grown and zone refined crystals. These values correspond to a boron to carbon ratio of \sim 4.1–4.2. This result differs from the results of the XEDS measurements which showed a carbon content of $17.0 \pm 0.8\%$ carbon content, which corresponds to a boron to carbon ratio of ~4.9 (see supplementary information). Discrepancies between these results may be due to lack of calibration samples used in the powder XRD technique. Raman spectroscopy (see supplementary information) of the polished surface also showed no signature of graphitic carbon inclusions [6,21,11].

Fig. 2 presents EBSD orientation maps of different boron carbide samples grown at varying growth rates, along the growth plane. These measurements show large crystalline regions hundreds of microns, as well as a significant portion of twinned regions. A clear twinning structure, with domains misoriented by 73°, is clearly seen. This is in agreement with previous TEM investigations of twin in B₄C [20,2]. For all runs performed at 10 mm/hr-20 mm/hr, we consistently observe $[0\ 0\ 1]_h$ orientation close to the growth direction, whereas for all runs performed at 5 mm/hr, various orientations have been observed such as [1 1 0]_h (see supplementary information). The preferential orientation of the crystal, and the twin-planes at the faster growth rates suggests a twin-plane mediated growth mechanism, as has also been observed in boron suboxide B₆O, a closely related rhombohedral crystal [23]. Additionally, the fraction of twin's density within the samples varied with the growth rate. A similar twin density fraction at 5 mm/hr and 10 mm/ hr growth rates decreased by about 50% at 20 mm/hr growth rate.

TEM investigations also revealed even finer planar and line defects (stacking faults (SFs) and associated partial dislocations (PDs)) in addition to the micron scale twins in the samples. An example of these defects is shown in Fig. 3 for a standard growth rate sample. Similar

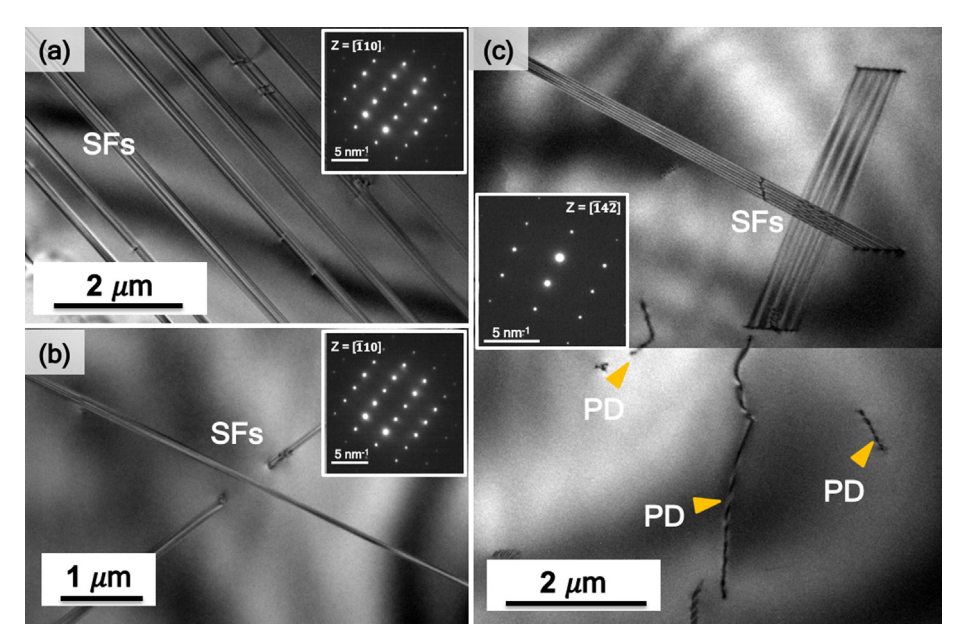


Fig. 3. TEM down-zone BF-micrographs present a non-uniform density of stacking faults (SFs) and associated partial dislocations (PDs) at three different locations in a standard growth rate sample. (a) Presents an array of high density of parallel SFs. (b-c) Show areas with relatively lower density of SFs and associated PDs.

observations were made on other samples grown at different growth rates. The average density of these stacking faults was found to be 1.3 $\,\pm\,$ 0.6 \times 10^{13} m $^{-2}.$

Significantly fewer impurities, as measured by GDMS, were found in the zone refined crystal compared to the directly as-grown crystal. Results show Mg, Al, and Fe were above the detection limit prior to zone refinement and were below the detection limit after (see supplementary information). Heavy metals were most affected by the zone refinement. The relatively high concentration of Si in crystal as compared to the starting material may be due to the inclusion of free silicon originating from the quartz tube that encloses the reaction.

Berkovich nanoindentation at 50mN loads showed results comparable to those in the literature on single-crystalline [10] and polycrystalline B_4C samples [12,4]. The hardness of the material perpendicular to the (0 0 1)h and (1 0 1)h planes were measured to be 41 \pm 1 GPa. The elastic modulus was measured to be 520 \pm 14 GPa.

The rocking curve and the map for a sample, shows a full-width half maximum (FWHM) of 530 arcsecs, which compares reasonably with high quality semiconductor substrates that typically show $\sim\!30\text{--}100$ arcsec (see supplementary information). This result confirms the orientation of the sample as previously characterized via EBSD (0 0 3)h as well as the high quality of the crystal.

4. Summary and conclusions

Using the LDFZ technique, high purity crystals of B_4C with large single crystal regions were produced. These materials were grown from un-oriented grains of polycrystalline B_4C . Samples were shown to be purified through the zone refining method. The single crystals of B_4C grown in this study contain a high density of symmetric twins that increase with growth speed and zone refinement. The carbon content of the material based on X-ray diffraction lattice parameter analysis was ~20% corresponding to a stoichiometry of B_4C . The preferred growth direction of the B_4C is the $(0\ 0\ 1)_h$ plane which occurs spontaneously during the growth. The elastic modulus along the $(0\ 0\ 1)_h$ and $(1\ 0\ 1)_h$ planes is $520\ \pm\ 14$ GPa using Berkovich indentation. The average density of the stacking faults is $1.3\ \pm\ 0.6\ \times\ 10^{13}\ m^{-2}$. The Berkovich hardness along the $(0\ 0\ 1)_h$ and $(1\ 0\ 1)_h$ planes is $41\ \pm\ 1$ GPa. The purity of the samples can be improved through zone refinement producing samples with purity comparable to that of semiconductors used

in industry. Rocking curve measurements confirm the high quality of the sample's lattice.

CRediT authorship contribution statement

Michael Straker: Methodology, Validation, Writing - original draft, Writing - review & editing, Visualization. Ankur Chauhan: Validation, Formal analysis, Writing - review & editing. Mekhola Sinha: Methodology, Writing - review & editing. W. Adam Phelan: Conceptualization, Methodology, Formal analysis, Writing - review & editing. M.V.S. Chandrashekhar: Conceptualization, Methodology, Validation, Formal analysis, Writing - original draft, Writing - review & editing. Kevin J. Hemker: Writing - review & editing, Supervision. Christopher Marvel: Conceptualization, Methodology, Writing - review & editing, Project administration, Funding acquisition. Michael Spencer: Validation, Formal analysis.

Declaration of Competing Interest

The authors declare that they have no known competing financial interests or personal relationships that could have appeared to influence the work reported in this paper.

Acknowledgements

Research was sponsored by the Army Research Laboratory and was accomplished under Cooperative Agreement Number W911NF-12-2-0022. The views and conclusions contained in this document are those of the authors and should not be interpreted as representing the official policies, either expressed or implied, of the Army Research Laboratory or the U.S. Government. The U.S. Government is authorized to reproduce and distribute reprints for Government purposes notwithstanding any copyright notation herein.

This material is based upon work supported by the Hopkins Extreme Materials Institute (HEMI), Extreme Science Internship Program (ESI), and the National Science Foundation (Platform for the Accelerated Realization, Analysis, and Discovery of Interface Materials (PARADIM)) under Cooperative Agreement No. DMR-1539918.

Appendix A. Supplementary material

Supplementary data to this article can be found online at https://doi.org/10.1016/j.jcrysgro.2020.125700.

References

- [1] T.L. Aselage, R.G. Tissot, Lattice constants of boron carbide, J. Am. Ceram. Soc. 75 (8) (1992) 2207–2212.
- [2] Q. An, W.A. Goddard III, K.Y. Xie, G. Sim, K.J. Hemker, T. Munhollon, M.F. Toksoy, R.A. Haber, Superstrength through nanotwinning, Nano Lett. 16 (12) (2016) 7573–7579
- [3] M. Beauvy, Stoichiometric limits of carbon-rich boron carbide phasesb, J. Less-Common Met. 90 (2) (1983) 169–175.
- [4] A. Chauhan, M.C. Schaefer, R.A. Haber, K.J. Hemker, Experimental observations of amorphization in stoichiometric and boron-rich boron carbide, Acta. Mater. 181 (2019) 207–215.
- [5] A. Chauhan, X. Sun, K.T. Ramesh, K.J. Hemker, Dynamic failure mechanisms of granular boron carbide under multi-axial high-strain-rate loading, Scr. Mater. 173 (2019) 125–128.
- [6] M. Chen, J.W. McCauley, J.C. LaSalvia, K.J. Hemker, Microstructural characterization of commercial hot-pressed boron carbide ceramics, J. Am. Ceram. Soc. 88 (7) (2005) 1935–1942.
- [7] M. Chen, J.W. McCauley, K.J. Hemker, Shock-induced localized amorphization in boron carbide, Science 299 (2003) 1563–1566.
- [8] J. Clayton, A. Tonge, A nonlinear anisotropic elastic-inelastic constitutive model for polycrystalline ceramics and minerals with application to boron carbide, Int. J. Solids Struct. 64–65 (2015) 191–207.
- [9] D. Dandekar, Elastic constants of calcite, J. Appl. Phys. 39 (1968) 2971.
- [10] V. Domnich, Y. Gogotsi, M. Trenary, T. Tanaka, Nanoindentation and Raman spectroscopy studies of boron carbide single crystals, Appl. Phys. Lett. 81 (20) (2002) 3783–3785.

- [11] V. Domnich, S. Reynaud, R. Haber, M. Chhowalla, Boron carbide: structure, properties, and stability under stress, J. Am. Ceram. Soc. 94 (11) (2011) 3605–3628.
- [12] D. Ge, V. Domnich, T. Juliano, E. Stach, Y. Gogotsi, Structural damage in boron carbide under contact loading, Acta Mater. 52 (13) (2004) 3921–3927.
- [13] I. Gunjishim, T. Akashi, G. Takashi, Thermoelectric properties of single crystalline B4C prepared by a floating zone method, Mater. Trans. 42 (7) (2001) 1445–1450.
- [14] T. Ito, T. Ushiyama, Y. Yanagisawa, Y. Tomioka, I. Shindo, A. Yanase, Laser-diode-heated floating zone (LDFZ) method appropriate to crystal growth of incongruently melting materials, J. Cryst. Growth 363 (2013) 264–269.
- [15] J.C. Lindon, G.E. Tranter, J.L. Holmes, Encyclopedia of Spectroscopy and Spectrometry, Academic Press, San Diego, 2000.
- [16] C. Marvel, K. Behler, J. LaSalvia, V. Domnich, R. Haber, M. Watanabe, M. Harmer, Extending ζ-factor microanalysis to boron-rich ceramics: Quantification of bulk stoichiometry and grain boundary composition, Ultramicroscopy 202 (2019) 163–172
- [17] K.J. McClellan, F. Chu, J.M. Roper, I. Shindo, Room temperature single crystal elastic constants of boron carbide, J. Mater. Sci. 36 (14) (2001) 3403–3407.
- [18] T. Nishinaga, P. Rudolph, Handbook of Crystal Growth, second ed., Elsevier, Amsterdam, 2015.
- [19] W. Pfann, Zone melting: this technique offers unique advantages I purification and in control of composition in various substances, Science 135(3509) (1962) 1101–1109
- [20] K. Xie, Q. An, M. Toksoy, J. McCauley, R. Haber, W. Goddard III, K. Hemker, Atomic-level understanding of "asymmetric twins" in boron carbide, Phys. Rev. Lett. 115 (17) (2015).
- [21] K.Y. Xie, K. Kulwelkar, R.A. Haber, J.C. Lasalvia, K.J. Hemker, Microstructural characterization of a commercial hot-pressed boron carbide armor plate, J. Am. Ceram. Soc. 99 (8) (2016) 2834–2841.
- [22] X. Yan, W. Li, T. Goto, M. Chen, Raman spectroscopy of pressure-induced amorphous boron carbide, Appl. Phys. Lett. 88 (13) (2006) 131905.
- [23] Z. Yu, X. Fu, J. Zhu, Revisiting the twin plane re-entrant edge growth mechanism at an atomic scale by electron microscopy, Cryst. Growth Des. 14 (9) (2014) 4411–4417.